

# FAST SUBSURFACE SAR SIMULATOR BASED ON GEOMETRICAL OPTICS

*Adel Elsherbini and Kamal Sarabandi*

Radiation Laboratory, University of Michigan, Ann Arbor, MI, USA.

## 1. INTRODUCTION

In previous work [1], we investigated the design of a two frequency synthetic aperture radar interferometer for estimating the sand layer thickness and the bedrock topography in deserts and arid areas. This was shown to be very useful in many applications such as oil field explorations, environmental studies and archaeological surveys. In order to test the inversion algorithm for different complex top surface scenarios, a fast subsurface SAR simulator is required. Such a simulator can also be used to perform subsurface focusing to further improve the accuracy of the height estimation. Based on scaled model measurements [2], it was found that geometrical optics-based ray launching provides a suitable approximation for the wave propagation through the sand on condition that the top sand surface undulations are much larger than the operating wavelength. Compared to conventional SAR simulators [3] where the path between the radar and the scattering centers is a straight line, subsurface SAR simulations are much more computationally intensive since the path is a straight line from the radar to the top surface incidence point then another straight line with a different slope from the incidence point to the subsurface scattering center requiring the solution of a set of nonlinear equations to determine the incidence point for each scattering center as well as the transmission coefficient for the used polarization(s). In this work, we exploit the fact that the top sand surface is relatively smooth to significantly enhance the speed of the subsurface SAR simulations. We also present a sample test scenario of a common sand dune and the use of the inversion algorithm developed in [1] to determine the subsurface height.

## 2. SUBSURFACE SAR FORMULATION

The raw baseband range-compressed SAR image is a function of the radar position,  $x_j$  and time,  $t$ . For a number of discrete targets, it can be expressed as:

$$F(x_j, t) = C_1 \sum_{i=1}^N \frac{A_i(x_j) \text{sinc} \left( B \left( t - \frac{2R_i(x_j)}{c} \right) \right) \exp \left( -\frac{2i\omega_0 R_i(x_j)}{c} \right)}{R_i(x_j)^2}$$

where,  $C_1$  is a constant that is dependent on the radar system parameters and the antenna gain,  $N$  is the number of scattering points in the scene,  $A_i(x_j)=A(x_j, x_i, y_i, z_i)$  is an amplitude and phase factor that is dependent on the antenna radiation pattern and the transmission coefficient through the sand,  $B$  is the operating bandwidth,  $c$  is the speed of light in free space,  $\omega_0$  is the center angular frequency and  $R_i(x_j)=R(x_j, x_i, y_i, z_i)$  is the electrical range to each target. The above relation does not take into account the dispersion due to the propagation through the sand since the sand dispersion is very small and can be neglected for sand layer thicknesses that are less than  $\sim 40\text{m}$ . For distributed targets, the summation becomes a 2D integration, this is useful for including the speckle and the decorrelation effects, but it will not be considered in this paper. The exponential term generates the phase history of each target (usually referred to as the Doppler history). Through this Doppler history, the image can be focused along the azimuth direction (the flight direction), through techniques such as back projection or omega-k algorithm by coherent summation at each pixel after correction for the phase history. The amplitude of the term  $A_i$ , performs a windowing effect on the Doppler history and thus limits the resolution, whereas its phase variation causes distortion to the Doppler history and should be minimized through careful antenna design and/or calibration.

The ray path for an arbitrary sand geometry is shown in Fig. 1. The direct method to form the raw SAR data (generate  $R_i(x_j)$  and  $A_i(x_j)$ ), is by solving the system of nonlinear equations describing the ray propagation through the sand surface for each target and each radar position. For a few number of targets, this approach is feasible. However, for large number of targets (or distributed targets), the process becomes extremely time consuming. Thus, we developed a much faster and relatively accurate technique which can efficiently generate the raw SAR data for large number of targets without the computational cost of solving a set of nonlinear equations. The approach can be summarized as follows: at each radar position, a ray is launched from the radar to the center of a sand surface facet. The ray is then refracted through the sand facet using geometrical optics and propagated through the sand until it intersects with one of the bedrock triangular facets. The intersection point is denoted  $(x_n, y_n, z_n)$ . This is done for each sand surface facet in the scene. At this stage we have  $R(x_j, x_n, y_n, z_n(x_n, y_n))$  and  $A(x_j, x_n,$

$y_n, z_n(x_n, y_n)$ ) over a nonuniform grid  $(x_n, y_n)$  on the bedrock. Then, simple 2D interpolation on non-uniform grid can be used to obtain  $R_i(x_j) = R(x_j, x_i, y_i, z_i(x_i, y_i))$  and  $A_i(x_j) = A(x_j, x_i, y_i, z_i(x_i, y_i))$ . This process is then repeated for each radar position. This technique is much faster since 2D interpolation is much less computationally intensive than solution of nonlinear equations and since, for most natural sand surfaces, the surface undulations are smooth, interpolation yields reasonably accurate estimations.

### 3. SIMULATION RESULTS

The SAR simulator is used to generate the raw data for testing the subsurface InSAR inversion algorithm. The used scenario is shown in Fig. 2. It consists of a *barchan* sand dune [4] with a crest height of 10 meters and an array of point targets at a depth of 20 meters beneath the surface. Two raw SAR images were generated for the scene using slightly different flight paths with a 100m baseline as shown in Fig. 2. The two images are then focused using the conventional back-projection SAR focusing algorithm and the focused SAR images are shown in Fig. 3 (a). The two images were then coregistered using conventional geometrical coregistration and the phase interferogram was generated. It should be noted that the point targets appear as continuous targets after performing the boxcar averaging on the complex interferogram. The phase is then unwrapped and the height was estimated using both the conventional InSAR and the proposed algorithm. The results are shown in Fig. 3 (b). Again, we can see that the proposed algorithm could accurately predict the bedrock height (with rms error  $< 0.5\text{m}$ ) whereas the conventional technique produced significant height errors. The RMS height error is mainly due to defocusing through the sand layer and coregistration errors.

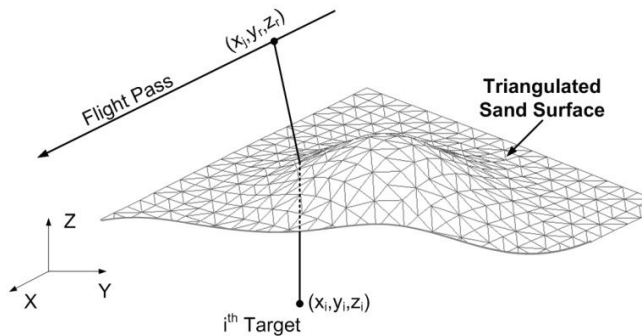


Fig. 1: 3D SAR Geometry.

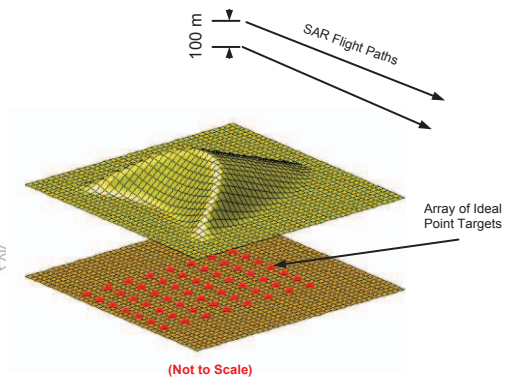
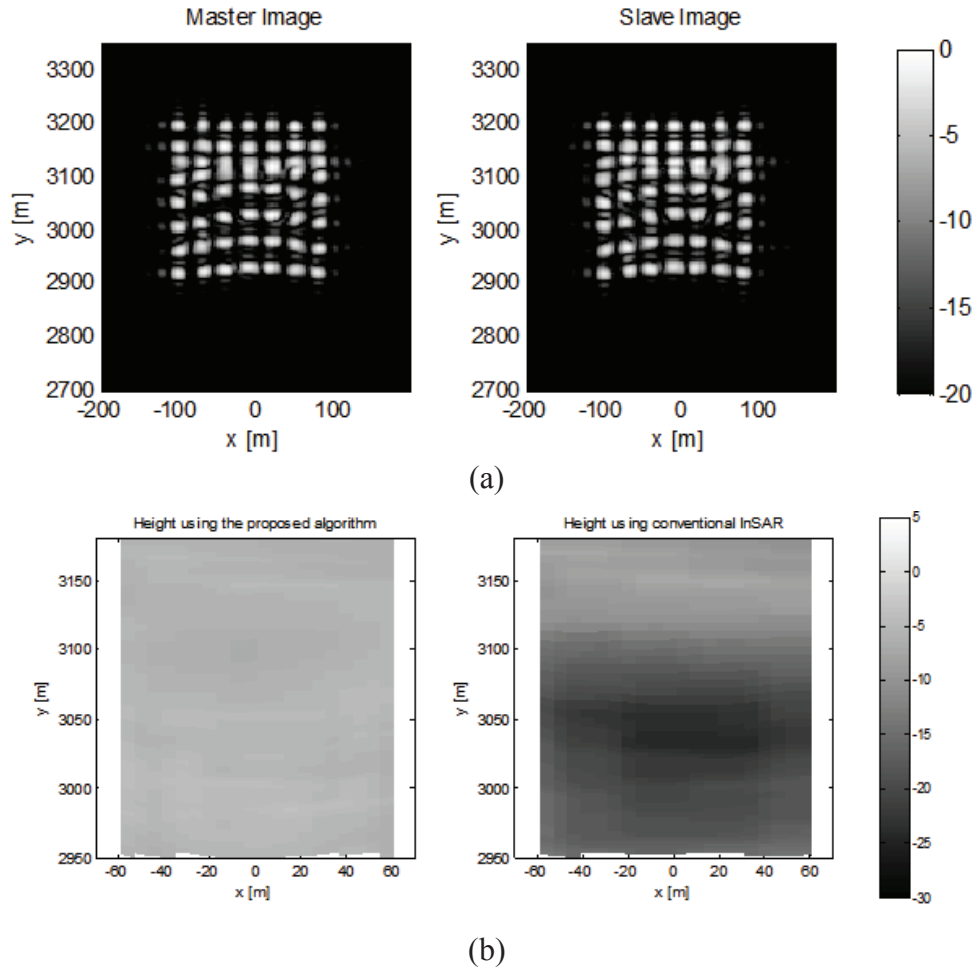


Fig. 2: 3D simulation scenario.



**Fig. 3: (a) The master and slave images for the InSAR simulation and (b) the calculated height using the proposed algorithm in [1] and using the conventional InSAR processing.**

## 11. REFERENCES

- [1] A. Elsherbini and K. Sarabandi, "Topography of Sand Covered Bedrock Using a Two-Frequency Airborne Interferometric SAR Measurements", 2009. IGARSS 2009, 12-17 July 2007, Cape Town, South Africa.
- [2] A. Elsherbini and K. Sarabandi, " Scaled Model For Sand-Covered Bedrock Mapping Interferometric SAR", 2009. IGARSS 2009, 12-17 July 2007, Cape Town, South Africa.
- [3] G. Franceschetti, M. Migliaccio, D. Riccio and G. Schirinzi, "SARAS: a synthetic aperture radar (SAR) raw signal simulator," *Geoscience and Remote Sensing, IEEE Transactions on* , vol.30, no.1, pp.110-123, Jan 1992.
- [4] V. Schwammle and H. J. Herrmann , "Geomorphology: Solitary wave behaviour of sand dunes", *Nature*, vol. 426, pp. 619-620, Dec. 2003.